

Interaction study of amino acid and volatile fatty acid on novel Kagome phosphorene nanotube - a DFT outlook

Bhuvaneshwari. R¹, Nagarajan. V¹, and R Chandiramouli¹

¹Shanmugha Arts Science Technology and Research Academy

May 6, 2020

Abstract

The deamination and decarboxylation of the Amino Acid – Asparagine results in Volatile Fatty Acid (VFA) – Lactate and Polyamine – Putrescine, which are culpable for the release of malicious odors into the atmosphere. In the present research, the bio-molecules (Asparagine, Lactate and Putrescine) are taken as primary molecules and are admitted to interact with the two-dimensional nanomaterial – Kagome form of Phosphorene nanotube (Kagome-PNT) by wielding the density functional theory mode. The conformational stability of the Kagome-PNT is affirmed with the help of formation energy and crystal orbital Hamiltonian population (COHP) analysis. Besides, the electronic features of the pure Kagome-PNT and bio-molecules interacted Kagome-PNT (complex) are estimated in addition to the COHP analysis on the complexes at the spot of bio-molecule interaction (hollow and triangle-spot). Further, the interaction features namely the binding energy, average energy gap alteration and Bader charge transfer are gauged so that our recommendation of wielding Kagome-PNT as a fundamental component in chemi-resistive based detector to sense the existence of bio-molecules (asparagine, lactate and putrescine) can be confirmed.

1. Introduction

A huge number of indispensable functions in human body are realized with the support of proteins, for which amino acids form the rudimentary building block. The distribution of amino acids in protein also regulates the grade and freshness of numerous foods. A notable operation that results in the emission of malicious aura in the outer atmosphere is anaerobic digestion, which is achieved by microbes on amino acids. Many compounds are produced as a result of amino acid catabolism [1], out of which we have concentrated on the two products – Volatile Fatty Acid (VFA) and amines. The deduction behind the catabolic reduction of amino acid to VFA and amines are accounted to be deamination and decarboxylation, respectively. Rappert and Muller [2] reported in their review article, which galvanized us to explore these three products – amino acid, VFA and amines. To be precise, the chief molecules chosen for the current work are asparagine (amino acid), lactate (VFA) and putrescine (amine). Asparagine is a non-essential amino acid, which is demanded by humans for the growth of brain. Some of the animal sources of asparagine are beef, eggs, poultry, diary, fish, whey and so on. Moreover, this amino acid is found to exist in potatoes, soybean, asparagus, corn, rye, maize, etc., [3, 4]. In concordance with the expected structure of amino acid, asparagine is reported to have an alpha-carboxylic acid group, alpha-amino group and a unique carboxamide sidechain (CONH₂). The molecular formula of asparagine, comprising the above-said groups is C₄H₈N₂O₃ and the vapor pressure is computed to be 4.8 x 10⁻⁸ mm Hg at 25 °C. Owing to the supreme nitrogen to carbon ratio, asparagine is accounted to be a productive choice for nitrogen transport and storage mechanism [5]. The possible sensing strategies previously employed for detecting asparagine amino acid are High Performance Liquid Chromatography (HPLC) [6] and MALDI/TOF-mass spectrometry (MS) [7]. The anaerobic deamination of the amino acid (present in vegetables and animals) lead to an intermediate product, VFAs which in general is wielded in a variety of industries manufacturing plastics, paints, fuels, textiles, pharmaceuticals and so on

[8]. The VFA – lactate ($C_3H_6O_3$) is regarded to be a bio-indicator owing to the physiological roles played by it in human body. The presence of lactate in blood, sweat, plasma and urine is utilized to witness the changes in the health of human body viz., sepsis [9], muscle fatigue, wound repair [10], acidosis, decubitus ulcers [11], etc. Besides, 0.5 to 2.0 mM is recorded to be the regular concentration range of lactate in the blood of human beings [12]. Moreover, higher the concentration of lactate in human body, higher is the risk associated with the human beings [13]. The formerly reported detection methods of lactate are HPLC, electrochemical-based, potentiometer-based and electro-chemiluminescent detection [14]. Microbial decarboxylation of amino acids leads to the release of a polyamine known as putrescine [15], which is noted to be a food quality indicator owing to the harmful impacts induced by it on the health of human beings upon the amplification of its level [16]. The polyamine with the molecular formula $C_4H_{12}N_2$ possesses hydrophobic methylene group and cationic demeanor. It is observed to be useful for the growth and proliferation of cells, bacteria and eukaryotes. In addition, certain physiological functions like collaboration of ribosomal subunits, alteration in the chromatin state, sustenance of tRNA structure, etc, are fulfilled using putrescine. To detect putrescine, several well-known techniques like HPLC, ion-exchange chromatography, capillary zone electrophoresis, colorimetric-based and capillary GC are used [17, 18]. The mode of sensing handled by us is of chemi-resistive type, which wields two-dimensional nanomaterials (2DNMs) as a fundamental component. The logic behind the preference of 2DNMs for the detection of amino acid, VFA and polyamine is that 2DNMs enjoys the advantage of extravagant surface area, which aids in intense physisorption of the bio-molecules. In addition, many marvellous attributes like malleability, optical transparency and pint-size of 2DNMs make them desirable. Moreover, the literary evidences recommend the exploitation of 2DNMs to identify the availability of bio-molecules – amino acid, VFA and polyamine. Some of the attestations include DNA nucleotide adsorption on graphene nanoribbons [19]; tyrosine and phenylalanine adsorption on graphene, graphene oxide and boron nitride [20]; histidine, aspartic acid, arginine, glycine, lysine, alanine, proline, glutamic acid, phenylalanine, tyrosine on graphene [21]; glycine, phenylalanine, histidine and glutamic acid on graphdiyne/graphene [22]; tryptophan, histidine, phenylalanine, tyrosine on graphene and single walled carbon nanotubes [23]. These documentations actuated us to find out a capable 2DNM to sense the presence of the amino acid – asparagine, VFA – lactate and polyamine – putrescine. One of the attractive 2DNM, which is known for its level-constrained band gap is phosphorene, a single layer of group-VA phosphorus (P) atoms. The tri-coordination of P atom together with its sp^3 type hybridization makes this 2DNM – phosphorene to have various kinds of conformations. Initially, α (black), β (blue), γ and δ -type of phosphorene were reported, followed by a variety of allotropes namely ζ , ϵ , λ (green), η , violet phosphorene and Kagome-form. Experimental realization of β -phosphorene and violet phosphorene by molecular beam epitaxy [24] and exfoliation [25] correspondingly encouraged the scientific community to persist many researches on this 2DNM [26-30]. Among the wide range of available allotropes, we have selected Kagome-form of Phosphorene (Kagome-P) as a fundamental component due to the spectacular characteristics exhibited by the material. The vigor demeanor of the 2DNM (Kagome-P) is observed owing to the geometry of the material, which follows both the α -P and β -P conformations. By perceiving the novel Kagome-P from side sight, α -P conformation is reckoned which is attributed to the interaction of a single P atom with two P atoms of the same level and one P atom of the second level. Also, every P atom in β -P conformation is being superseded by a triangle of P atoms. Experimental realization of Kagome-P can be carried out through polymerization mechanism [31] and compressive in-plane strain-based derivation mechanism (from β -P) [32]. Moreover, appealing attributes of Kagome-P like desirable absorption coefficient (10^5 cm^{-1}), wide-ranging band gap and strain-based band gap transition prepare the 2DNM to be operated in many optoelectronic devices. We studied the sensing properties of phosphorene nanotubes and nanosheets to vapors [33-37]. The ability of the 2DNM to take various forms like nanosheet, nanotube, nanoribbon, etc, without losing its stable 2D nature [38] along with the above-stated fascinating points impelled us to investigate the interaction of the bio-molecules – amino acid (asparagine), VFA (lactate) and polyamine (putrescine) on the Kagome-form of phosphorene nanotube (Kagome-PNT).

2. Estimation details

The density functional theory mode is adopted to carry out the investigation on the potentiality of the

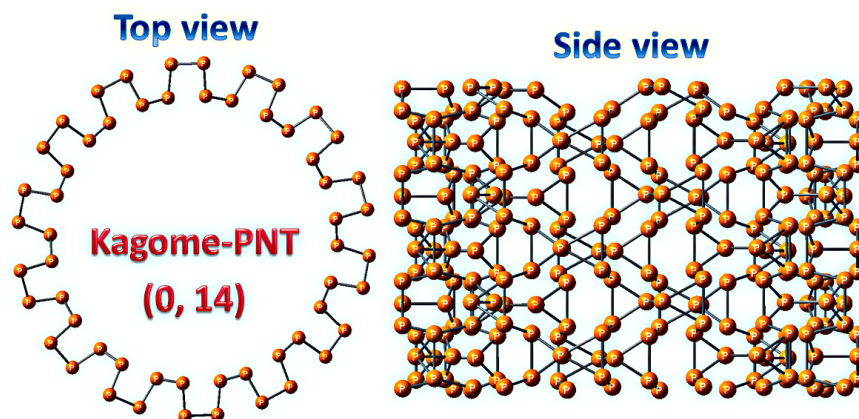
2DNM – Kagome-form of Phosphorene nanotube (Kagome-PNT) to be used as a fundamental component in chemi-resistive based sensor to detect the malicious aura producing bio-molecules – asparagine (amino acid), lactate (VFA) and putrescine (polyamine). The software package facilitating the scrutinization on Kagome-PNT is SIESTA [39]. The perfect conformation of the fundamental component is accomplished by converging the atomic forces on the constituent phosphorus atoms to $0.001 \text{ eV}/\text{\AA}$ and the energy convergence is adjusted to 10^{-6} eV . For the geometrical optimization, Grimme’s DFT-D2 correction is used while choosing significance of van der Waals interaction [40]. The kinetic-energy cut-off is set to 500 eV . The exploration on the conformational and electronic features of the pure Kagome-PNT and bio-molecules interacted Kagome-PNT is implemented under the framework of GGA-B3LYP exchange-correlation functional. The conformational stability of Kagome-PNT is verified using the formation energy. Besides, bonding and antibonding aspects between Kagome-PNT and target molecules are studied with regard to Crystal Orbital Hamiltonian Population (COHP) analysis [41]. The factors Density of states (DOS) spectrum and Band Structure under electronic features are explored for the pure and bio-molecules interacted Kagome-PNT after the sampling of Brillouin zones at $1 \times 1 \times 25$ are finalized. Moreover, double zeta polarization basis set and a vacuum padding of 16 \AA are fulfilled following which the interaction features namely the binding energy, average energy gap alteration and Bader charge transfer are gauged.

3. Outcome and elaboration

3.1 Conformational and electronic features of Kagome-Phosphorene nanotube

The bulk form of Kagome phosphorene nanosheet is belongs to the space group P-2M1 (164). The optimized lattice constant for single layer Kagome phosphorene nanosheet is computed to be $a=b=5.517 \text{ \AA}$, which is validated with previous reports (5.52 \AA [32]). Further, the bond distance among phosphorous atoms in Kagome phosphorene is found to be 2.24 \AA . A single layer of Kagome-form of phosphorene that is encompassing both the α -P and β -P form in its skeletal structure is preferred for the present research. The above optimized Kagome phosphorene then wrapped around with a chiral index (0,14) so that the Kagome-form of Phosphorene nanotube is formed (Kagome-PNT). The fundamental component of the current research – Kagome-PNT is pictorially displayed in Fig. 1. Two views are represented – one is an exact top sight which is portraying the α -P form (puckered structure) and another one is side sight which is depicting the triangle of P atoms in two levels (upper and lower).

Fig. 1 Optimized structure of Kagome-PNT.



Since the structural clarification for the fundamental component is provided, the conformational stability of the material is figured out through formation energy. The equation necessary to compute the formation

energy is given underneath [42, 43].

$$E_{\text{Form}} = (1/s)[E(\text{Kagome} - \text{PNT}) - sE(P)]$$

The factors handled in the calculating formation equation (E_{Form}) are the energy of the fundamental component $-E(\text{Kagome-PNT})$, procurable number of phosphorus (P) atoms in the fundamental component - 's' and energy of a single P atom $-E(P)$. By wielding the aforementioned parameters, the formation energy is assessed to be -3.883 eV per atom. The non-positive measure of E_{Form} verifies the conformational stability of the fundamental component. This is ascribed to the complex conformation of Kagome-PNT that follows the local co-ordination of α -P and global symmetry of β -P form [44]. In addition, to verify the dynamical stability of chief component Kagome-PNT, phonon-bands-spectrum is plotted as shown in Fig. 2. It is revealed that there is no imaginary-frequency noticed in the phonon spectrum, confirming the dynamical-stability of Kagome-PNT.

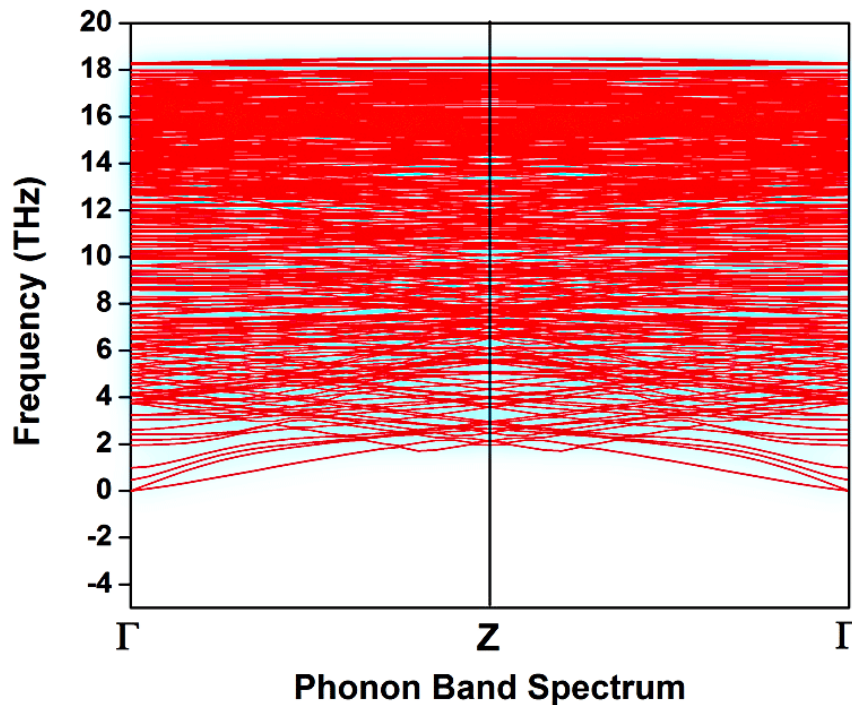


Fig. 2 Phonon band spectrum of Kagome-PNT.

As the structural and dynamical durability of the fundamental component is affirmed, the electronic features for the pure Kagome-PNT are explored. The first feature to assess under the electronic features is Band structure, which is wielded to express the energy band gap in terms of allowed and banned bands throughout the symmetry points [45, 46]. Then, the second feature, which also expresses the energy band gap through Fermi energy level is Density of States (DOS) spectrum. Besides, the count of usable states where the electrons can prevail can be outlined from DOS spectrum. These two features are plotted for the pure Kagome-PNT and represented in Fig. 3. The Fermi energy level (E_F) for the pure Kagome-PNT is reckoned to be -3.337 eV and the energy gap is ciphered to be 0.805 eV along the gamma (Γ) point. A feeble decrease in the energy gap is noticed upon comparison to the formerly performed calculations by Yu et al [47] (PBE-based). This can be rationalized due to the nanotube form of Kagome-Phosphorene, the geometry of which in general reduces the energy gap. Moreover, the energy gap is also reckoned from the DOS spectrum (between -3 and -4 eV, which upon closer examination will lead to -3.337 eV). A greater number of states for electron

accommodation is apprehended throughout the energy bands. Further, the subsistence of sharp peaks near the Fermi energy level favors the proposition of adopting Kagome-PNT as a chemi-resistive based detector.

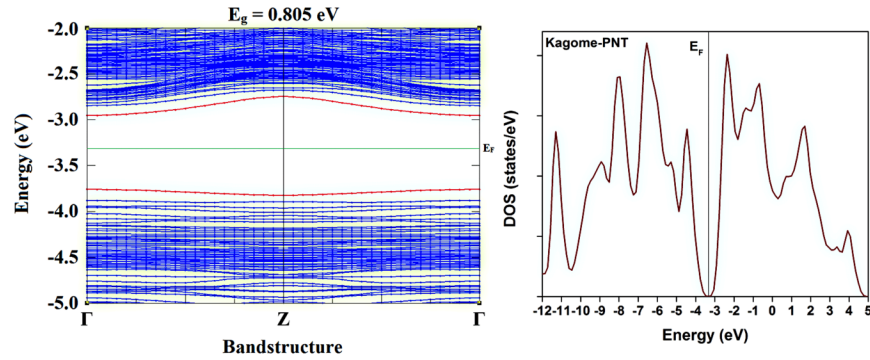


Fig. 3 Band structure and DOS maps of Kagome-PNT.

Another significant parameter discussed here is Crystal Orbital Hamiltonian Population (COHP) [48], which is evaluated to understand the bonding and antibonding bestowment towards a bond (between a couples of subjected atoms) of the fundamental component with respect to the Band structure energy. Fig. 4 sketches the COHP estimated for the bond between two P atoms of pure Kagome-PNT. It can be unmistakably understood from the diagram that the valence band exhibits a larger amount of bonding characteristics and a feeble measure of antibonding characteristics. Also, the domination of antibonding characteristic is seen throughout the conduction band in addition to the expression of non-bonding characteristic near the Fermi energy level as depicted in Fig. 4. This symbolizes the stability of the fundamental component in terms of bond strength.

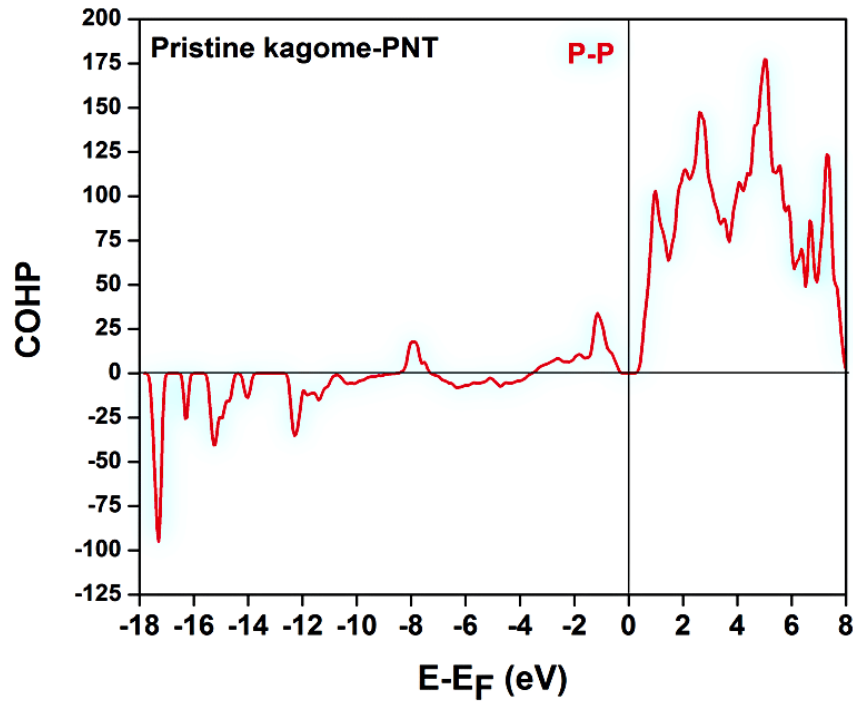


Fig. 4 COHP analysis for pristine Kagome-PNT.

Now, the primary bio-molecules – amino acid (asparagine), VFA (lactate) and polyamine (putrescine) are admitted to interact with the fundamental component – Kagome-PNT at two distinct spots – hollow and triangle. This form of interaction is performed based on the work of Ralph H Scheicher [49, 50], where the spots with small binding energy is chosen as global minima spot. The interaction of asparagine, lactate and putrescine on Kagome-PNT are specified as Complex X, Y and Z (1-hollow; 2-triangle) to enable pleasant interpretation for the readers and are illustrated in Fig. 5 (a) – (c).

Fig. 5 (a) Adsorption of asparagine on hollow site (complex X1) and triangle site (complex X2) of Kagome-PNT.

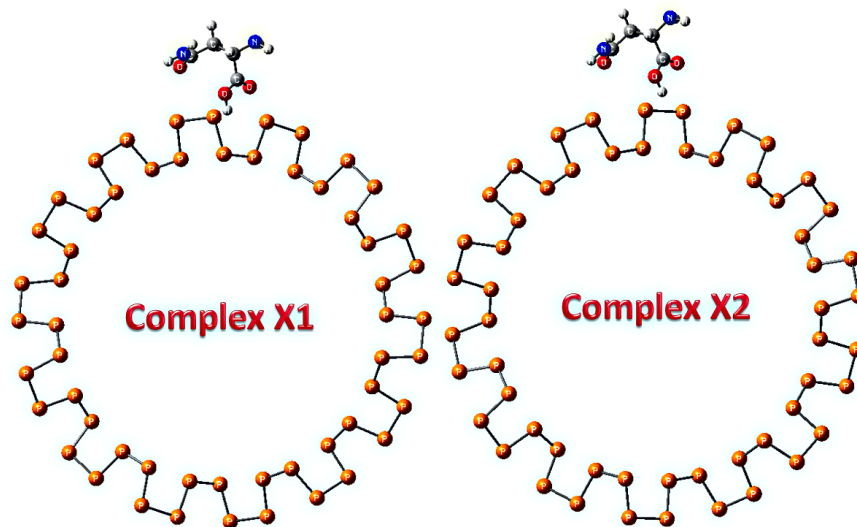


Fig. 5 (b) Adsorption of lactate on hollow site (complex Y1) and triangle site (complex Y2) of Kagome-PNT.

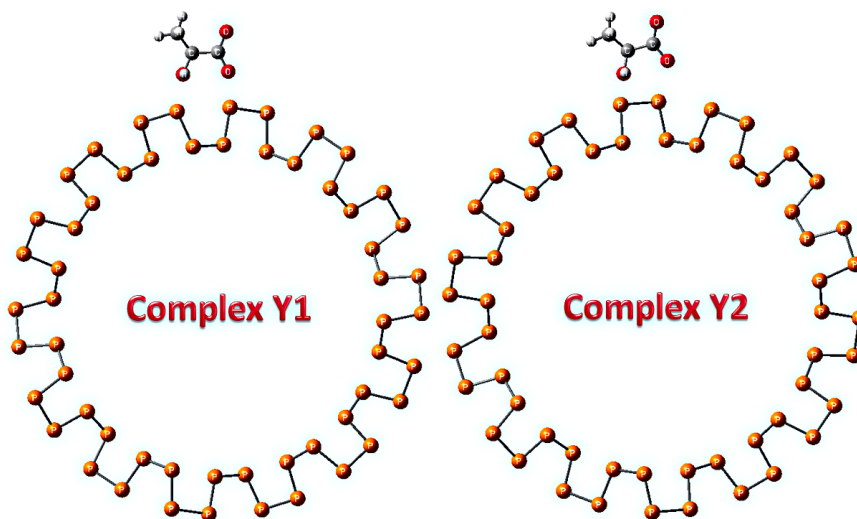
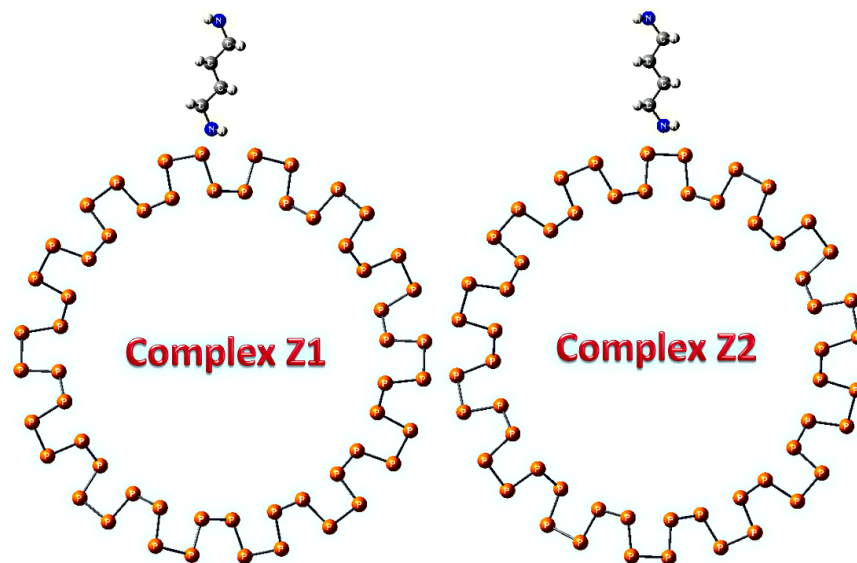


Fig. 5 (c) Adsorption of putrescine on hollow site (complex Z1) and triangle site (complex Z2) of Kagome-PNT.



The electronic features, namely the Band structure and DOS spectrum are determined for the bio-molecules interacted Kagome-PNT and are outlined in Fig. 6 (a) – (f). The Band structure yields the Fermi energy level (E_F) for complex X1, X2 as -3.568 eV and -3.584 eV; for complex Y1, Y2 as -4.165 eV and -4.109 eV; for complex Z1, Z2 as -3.570 eV and -3.533 eV. On the same note, the energy gap values are deduced to be 1.163 eV for Complex X1 and X2; 1.097 eV and 1.053 eV for complex Y1 and Y2; 1.159 eV and 1.163 eV for Complex Z1 and Z2. It can be clearly comprehended that the energy gap values are augmented for all the bio-molecules interacted complexes [51-53]. This enhancement in the energy gap value when compared to the pure Kagome-PNT in turn influences the conductivity of the nanotube i.e., it decreases the current flowing through the nanotube. Besides, more number of peaks is perceived throughout the energy interval of DOS spectrum when compared to the pure Kagome-PNT and modification is also noticed among the bio-molecules interacted complexes.

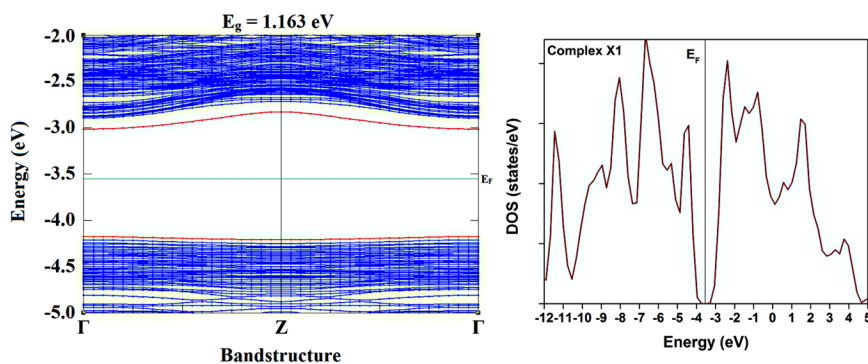


Fig. 6 (a) Bandstructure and DOS plot – complex X1.

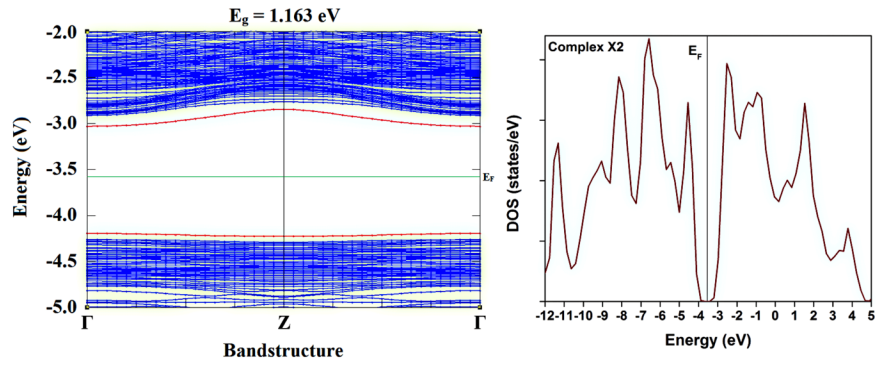


Fig. 6 (b) Bandstructure and DOS plot – complex X2.

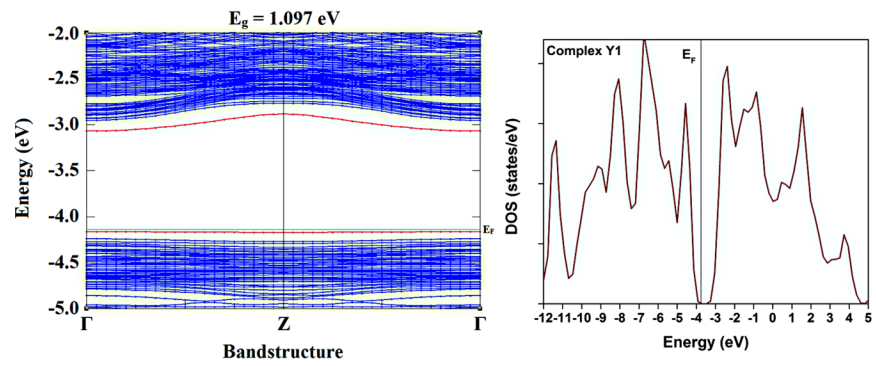


Fig. 6 (c) Bandstructure and DOS plot – complex Y1.

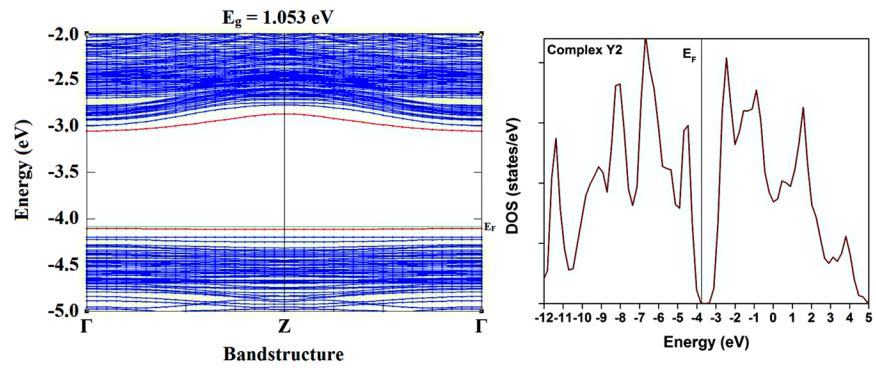


Fig. 6 (d) Bandstructure and DOS plot – complex Y2.

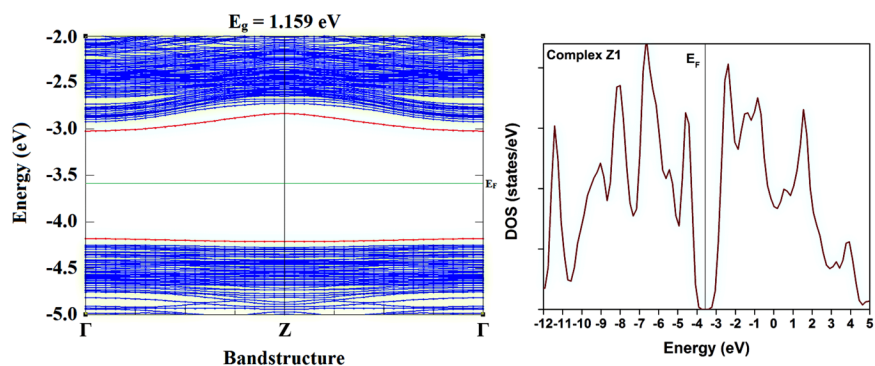


Fig. 6 (e) Bandstructure and DOS plot – complex Z1.

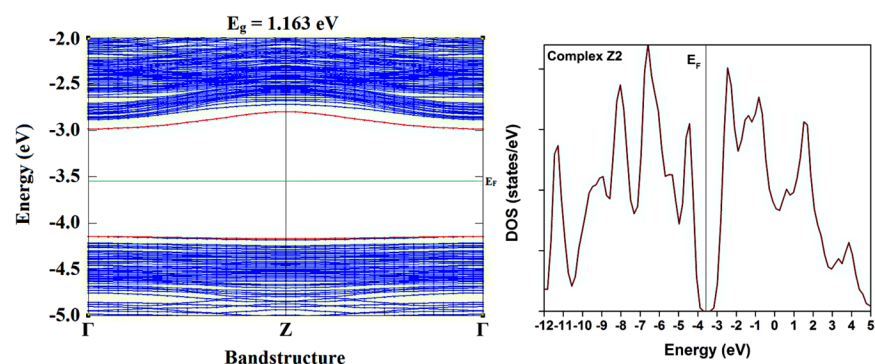


Fig. 6 (f) Bandstructure and DOS plot – complex Z2.

The availability of a greater number of states enunciates the happening of bio-molecule interaction on Kagome-PNT. As the alteration in the electronic features for the bio-molecules interacted complexes are studied, COHP analysis is implemented and presented in Fig. 7 (a) – (c). A drastic variation can be reckoned for each bio-molecule interaction at specific site. In case of Complex X1 and X2, since the interaction of asparagine is made through the oxygen (O) atom on Kagome-PNT, COHP is calculated for P-O bond. Moreover, the VFA – lactate and polyamine – putrescine are admitted to interact with Kagome-PNT through O and N atom respectively, so COHP calculations for Complex Y and Z are performed on P-O and P-N bonds correspondingly. For complex X1, though the bonding bestowment is observed near -8.3 eV (valence band) and 6.4 eV (conduction band) in the form of spikes, maximum bestowment comes from antibonding, especially near the Fermi energy level (E_F). However, for complex X2, a greater absolute value of COHP (-3.3) is noticed near 14 eV (conduction band) contributing to bonding attribute and the antibonding bestowment is observed to be trivial. For complex Y1, an equal number of bonding (negative COHP measure) and antibonding (positive COHP measure) is reckoned. Yet, the antibonding characteristic is found to be dominant for complex Y2 with a fewer spike indicating bonding nature at higher energy levels (8 to 12 eV). In case of complex Z1 and Z2, bonding features are found predominant at higher energy levels (7 to 12 eV – conduction band) along with the prevalence of antibonding characteristics throughout the valence band and at lower energy levels of conduction band. Although the variation in the distribution of bonding and antibonding attributes for the complexes X, Y and Z are figured out through the COHP plot, the non-bonding characteristic at the Fermi energy level (E_F) remains the same for all the bio-molecule interacted complexes. The electronic features elaborated so far ensures our preference of Kagome-PNT to sense the molecules – asparagine, lactate and putrescine.

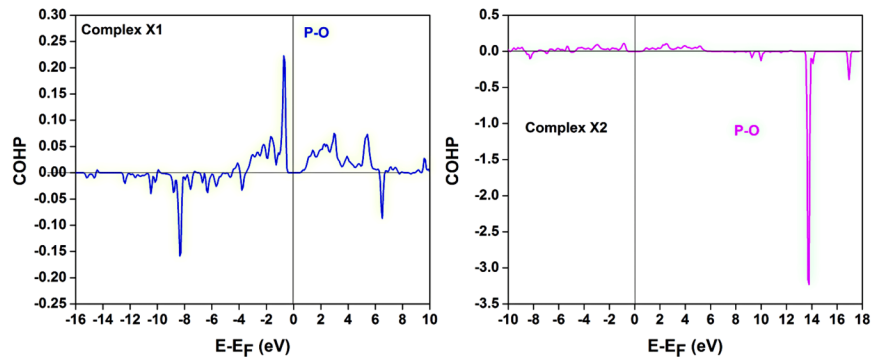


Fig. 7 (a) COHP analysis for complex X1 & X2.

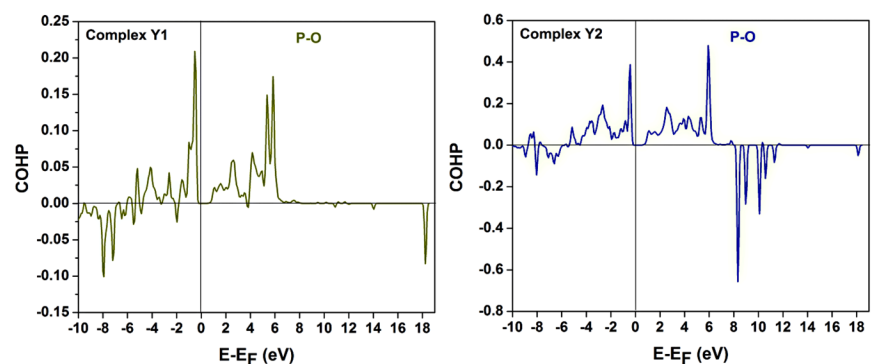


Fig. 7 (b) COHP analysis for complex Y1 & Y2.

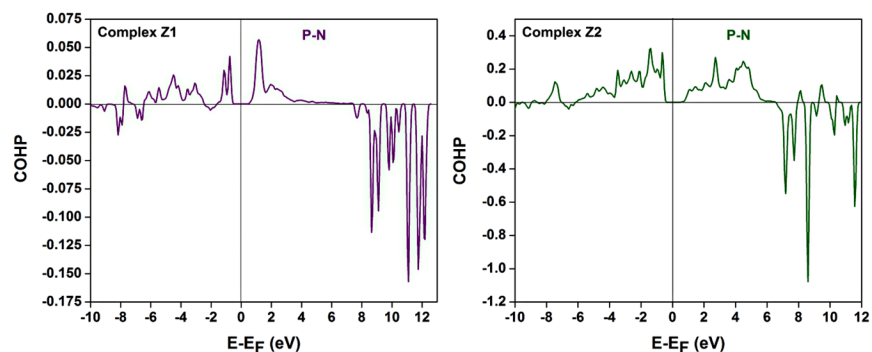


Fig. 7 (c) COHP analysis for complex Z1 & Z2.

3.2 Interaction features of bio-molecules on Kagome-PNT

The critical factors under the interaction features namely, the binding energy (E_{Bind} eV), average energy gap alteration (E_g^a %) and Bader charge transfer (Q e) are evaluated now to further emphasize our proposition of using Kagome-PNT as a fundamental component to detect the bio-molecules (amino acid, VFA and polyamines). Table 1 represents the interaction features along with the Fermi energy level and energy gap. The formula involved in calculating the binding energy (E_{Bind}) is furnished underneath [54-58].

$$E_{\text{Bind}} = E(\text{Kagome} - \text{PNT}|\text{Biomolecule}) - E(\text{Kagome} - \text{PNT}) - E(\text{Biomolecule}) + E(\text{BSSE})$$

The parameters encompassing the equation to find E_{Bind} are the energy of the complex $E(\text{Kagome-PNT}|\text{Biomolecules})$, energy of the fundamental component $E(\text{Kagome-PNT})$, energy of the biomolecule interacted $E(\text{Biomolecule})$ and energy necessary to determine the Basis set superposition error $E(\text{BSSE})$. The last term is enclosed in the formula specified above in order to remove the overlapping impacts.

Table 1. Binding energy (E_{bind}), Bader charge transfer (Q), Fermi level energy (E_{F}), energy gap (E_{g}) and average energy gap alteration (E_{g}^{a}) of target molecule interacted Kagome-PNT.

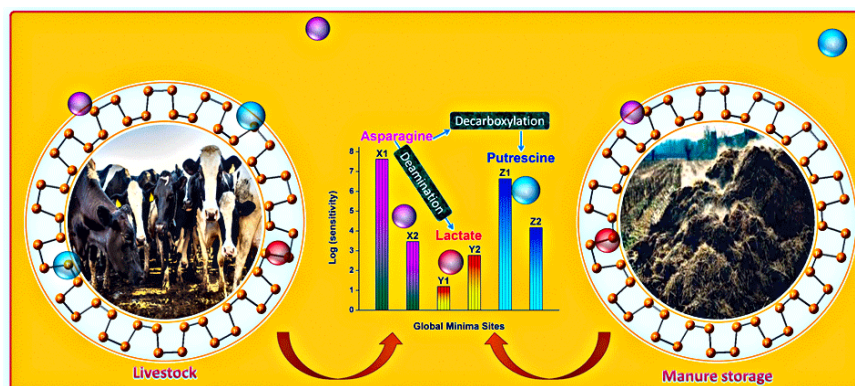
Kagome-PNT and complexes	E_{bind} (eV)	Q(e)	E_{F} (eV)	E_{g} (eV)	E_{g}^{a} (%)
Kagome-PNT	-	-	-3.337	0.805	-
complex X1	-0.071	-0.104	-3.568	1.163	44.47
complex X2	-0.269	0.072	-3.584	1.163	44.47
complex Y1	-0.146	0.298	-4.165	1.097	36.27
complex Y2	-0.200	0.263	-4.109	1.053	30.81
complex Z1	-0.835	0.023	-3.570	1.159	43.98
complex Z2	-0.321	-0.183	-3.533	1.163	44.47

The measure of binding energy computed for the complex X1 and X2 are -0.071 eV and -0.269 eV; for the complex Y1 and Y2 are -0.146 eV and -0.2 eV; for the complex Z1 and Z2 are -0.835 eV and -0.321 eV correspondingly. Among the values figured out, it can be heeded that the absolute measure of binding energy for Complex Z are higher relative to the other complexes. This reveals the fruitful interaction of putrescine on the Kagome-PNT. Yet, the reversibility of the fundamental component upon the putrescine interaction is limited to some extent compared to the other molecules' interaction. For asparagine and lactate interaction on Kagome-PNT, reversible demeanor of the fundamental component is simple if they are admitted to interact at the hollow-spot, whereas efficient interaction can be visualized for the triangle-spot interaction of asparagine and lactate. In addition, the non-positive measure of E_{Bind} for all the complexes betokens the effortless interaction of the bio-molecules on the fundamental component [59]. Moreover, owing to the value of E_{Bind} (which is lower than unit magnitude), physisorption form of interaction is reckoned for all the complexes.

The desirable spot of bio-molecule interaction on fundamental component can be gauged from average energy gap alteration (E_{g}^{a} %) [60-63]. For complex X1 and X2, 44.47 % is observed; for complex Y1 and Y2, 36.27% and 30.81% is noticed; for complex Z1 and Z2, 43.98% and 44.47% is perceived. A noble alteration is recognized for all the bio-molecules (amino acid, VFA and polyamine) interaction on the fundamental component, which testifies the utility of Kagome-PNT to detect the same. Owing to the same response induced by Kagome-PNT to asparagine for both the hollow and triangle-spot, identical E_{g}^{a} % is witnessed. For the other molecules' (lactate and putrescine) interaction on the fundamental component, close response is discerned. The transmission of charges between the fundamental component and the bio-molecules can be acknowledged with the help of Bader charge transfer (Q) [64-68]. The magnitude of Q estimated for complex X1 and X2 are -0.104 e and 0.072 e; for complex Y1 and Y2 are 0.298 e and 0.263 e; for complex Z1 and Z2 are 0.023 e and -0.183 e, correspondingly. A notable positive transfer of charges is seen for lactate interaction on Kagome-PNT (complex Y1 and Y2), which specifies the orientation of charge transmission from the molecule to the fundamental component. In case of complex X1 (asparagine interaction on hollow-spot of Kagome-PNT), the carboxylic group of the amino acid interacts with the P atom of the fundamental component in such a way that a negative Q is measured for this particular spot-interaction. On the same note, for complex Z2 (putrescine interaction on triangle-spot of Kagome-PNT), the amine group of the polyamine makes the value of Q non positive, which means that the charge transmission occurs from the fundamental component to the molecule. Fig. 8 depicts the perception on sensing response of Kagome-PNT towards amino acids and its products. Overall, the interaction features of the bio-molecules (asparagine, lactate and putrescine) on

the Kagome-PNT signifies the employment of the same as fundamental component to sense the availability of the target bio-molecules.

Fig. 8 Perception on sensing response of Kagome-PNT towards amino acids and its products



4. Inference

To sum up, it is evident that the unpleasant odor released into the outer atmosphere is due to the microbial deamination and decarboxylation of amino acid, asparagine into VFA – lactate and polyamine – putrescine, respectively. We utilized Kagome form of Phosphorene nanotube (Kagome-PNT) for sensing the presence of amino acid and its products. Density functional theory mode is adopted in the present investigation and the conformational stability of Kagome-PNT is affirmed with the help of formation energy. Besides, the factors Density of states (DOS) spectrum and Band Structure under electronic features are evaluated for the pure Kagome-PNT and the bio-molecules (asparagine, lactate and putrescine) interacted Kagome-PNT. In addition, COHP analysis is carried out for the bio-molecules interacted complexes at the spot of interaction (between the Phosphorus atom and the interacting atom of the molecule). Moreover, the interaction features namely, the Binding energy, average energy gap alteration and Bader charge transfer are gauged for the bio-molecules interacted Kagome-PNT (both hollow and triangle-spot interaction). The deduction made from the current scrutinization is that the Kagome-form of phosphorene nanotube can be effortlessly employed as a fundamental component in chemi-resistive based sensor to detect the presence of the bio-molecules – asparagine, lactate and putrescine.

Acknowledgement

The authors wish to express their sincere thanks to Nano Mission Council (No.SR/NM/NS-1011/2017(G)) Department of Science & Technology, India for the financial support.

References

- [1] R.I. Mackie, P.G. Stroot, V.H. Varel, *J. Anim. Sci.* **1998** , 76 , 1331.
- [2] S. Rappert, R. Müller, *Waste Manag.* **2005** ,25 , 887.
- [3] N. Muttucumar, A.J. Keys, M.A.J. Parry, S.J. Powers, N.G. Halford, *Planta.* **2014** , 239 , 161.
- [4] G. Lohaus, M. Büker, M. Hußmann, C. Soave, H.W. Heldt, *Planta.* **1998** , 205 , 181.
- [5] G.M. Coruzzi, *Arab. B.* **2003** , 2 , e0010.
- [6] C. Bai, C.C. Reilly, B.W. Wood, *Anal. Chem. Methods Appl.* **2011** , 278.
- [7] D. Kameoka, T. Ueda, T. Imoto, *J. Biochem.* **2003** ,134 , 129.
- [8] J. Jiang, Y. Zhang, K. Li, Q. Wang, C. Gong, M. Li, *Bioresour. Technol.* **2013** , 143 , 525.

- [9] J. Bakker, P. Gris, M. Coffernils, R.J. Kahn, J.L. Vincent, *Am. J. Surg.* **1996** , 171 , 221.
- [10] L.B. Gladden, *J. Physiol.* **2004** , 558 , 5.
- [11] P.J. Derbyshire, H. Barr, F. Davis, S.P.J. Higson, *J. Physiol. Sci.* **2012** , 62 , 429.
- [12] L. Rassaei, W. Olthuis, S. Tsujimura, E.J.R. Sudhölter, A. Van Den Berg, *Anal. Bioanal. Chem.* **2014** , 406 , 123.
- [13] S.E. Allen, J.L. Holm, *J. Vet. Emerg. Crit. Care.***2008** , 18 , 123.
- [14] X. Cai, J. Yan, H. Chu, M. Wu, Y. Tu, *Sensors Actuators, B Chem.* **2010** , 143 , 655.
- [15] B.W. Straub, M. Kicherer, S.M. Schilcher, W.P. Hammes, *Z. Lebensm. Unters. Forsch.* **1995** , 201 , 79.
- [16] S. Baixas-Nogueras, S. Bover-Cid, M.T. Veciana-Nogués, A. Mariné-Font, M.C. Vidal-Carou, *J. Food Prot.* **2005** , 68 , 2433.
- [17] M. Venza, M. Visalli, D. Cicciu, D. Teti, *J. Chromatogr. B* **2001** , 757 , 111.
- [18] W. Zhang, Y. Tang, J. Liu, L. Jiang, W. Huang, F.W. Huo, D. Tian, *J. Agric. Food Chem.* **2015** , 63 , 39.
- [19] E.C. Lee, *Appl. Phys. Lett.* **2012** , 100 , 2.
- [20] S.S.K. Mallineni, J. Shannahan, A.J. Raghavendra, A.M. Rao, J.M. Brown, R. Podila, *ACS Appl. Mater. Interfaces.***2016** , 8 , 16604.
- [21] S.J. Rodríguez, E.A. Albanesi, *Phys. Chem. Chem. Phys.***2019** , 21 , 597.
- [22] X. Chen, P. Gao, L. Guo, S. Zhang, Graphdiyne as a promising material for detecting amino acids, *Sci. Rep.* **2015** , 5 , 1.
- [23] C. Rajesh, C. Majumder, H. Mizuseki, Y. Kawazoe, *J. Chem. Phys.* **2009** , 130 , 124911.
- [24] J. Xu, J. Zhang, H. Tian, H. Xu, W. Ho, M. Xie, *Phys. Rev. Materials* **2017** , 1 , 061002.
- [25] L. Zhang, H. Huang, B. Zhang, M. Gu, D. Zhao, X. Zhao, L. Li, J. Zhou, K. Wu, Y. Cheng, J. Zhang, *Angew. Chem. Int. Ed.***2020** , 59 , 1074.
- [26] S. Zhang, M. Xie, F. Li, Z. Yan, Y. Li, E. Kan, W. Liu, Z. Chen, H. Zeng, *Angew. Chem. Int. Ed.* **2016** , 55 , 1666.
- [27] S. Zhang, Z. Yan, Y. Li, Z. Chen, H. Zeng, *Angew. Chem.***2015** , 127 , 1.
- [28] S. Zhang, S. Guo, Z. Chen, Y. Wang, *Chem. Soc. Rev.***2017** , 47 , 982.
- [29] Y. Zhou, M. Zhang, Z. Guo, L. Miao, S.T. Han, Z. Wang, X. Zhang, H. Zhang, Z. Peng, *Mater. Horizons.* **2017** , 4 , 997.
- [30] S. Guo, Y. Zhang, Y. Ge, S. Zhang, H. Zeng, H. Zhang, *Adv. Mater.* **2019** , 31 , 1.
- [31] R.O. Jones, D. Hohl, *J. Chem. Phys.* **1990** , 92 , 6710.
- [32] P.J. Chen, H.T. Jeng, *Sci. Rep.* **2016** , 6 , 1.
- [33] V. Nagarajan, R. Chandiramouli, *Chem. Phys.***2020** , 535 , 110782.
- [34] P.C. Sruthy, V. Nagarajan, R. Chandiramouli, *J. Mol. Graph. Model.* **2020** , 97 , 107566.
- [35] J.P. Maria, R. Bhuvanewari, V. Nagarajan, R. Chandiramouli, *J. Mol. Graph. Model.* **2020** , 95 , 107505.
- [36] J. Princy Maria, R. Bhuvanewari, V. Nagarajan, R. Chandiramouli, *Mol. Phys.* **2020** , 8976 , 1737744.

- [37] R. Bhuvaneswari, J. Princy Maria, V. Nagarajan, R. Chandiramouli, *Chem. Phys. Lett.* **2020** , 747 , 137353.
- [38] J. Guan, Z. Zhu, D. Tománek, *Phys. Rev. Lett.* **2014** , 113 , 1.
- [39] M. Soler, E. Artacho, J.D. Gale, A. Garc, J. Junquera, P. Ordej, S. Daniel, *J. Phys.: Condens. Matter* **2002** ,14 , 2745.
- [40] S. Grimme, *Adv. Rev. WIREs Comput Mol Sci* **2011** ,1 , 211.
- [41] R. Sabitha, V. Nagarajan, R. Chandiramouli, *ChemistrySelect* **2020** , 5 , 3398.
- [42] R. Bhuvaneswari, V. Nagarajan, R. Chandiramouli, *Phys. B Condens. Matter.* **2020** , 586 , 412135.
- [43] R. Bhuvaneswari, J.P. Maria, V. Nagarajan, R. Chandiramouli, *Comput. Theor. Chem.* **2020** , 1176 , 112751.
- [44] J. Zhu, C. He, Y. Zhao, B. Fu, *J. Mater. Chem. C* **2020** , 8 , 2732.
- [45] B. Amin, T.P. Kaloni, U. Schwingenschlögl, *RSC Adv.* **2014** , 4 , 34561.
- [46] T.P. Kaloni, *J. Phys. Chem. C.* **2014** ,118 , 25200.
- [47] G. Yu, L. Jiang, Y. Zheng, *J. Phys.: Condens. Matter* **2015** , 27 , 255006.
- [48] S. Kiruthika, H. Fjellvåg, P. Ravindran, *J. Mater. Chem. A.* **2019** , 7 , 6228.
- [49] R.G. Amorim, R.H. Scheicher, *Nanotechnology.* **2015** , 26 , 154002.
- [50] S. Mukhopadhyay, R.H. Scheicher, R. Pandey, S.P. Karna, *J. Phys. Chem. Lett.* **2011** , 2 , 2442.
- [51] H. Sajid, K. Ayub, M. Arshad, T. Mahmood, *Comput. Theor. Chem.* **2019** , 1163 , 112509.
- [52] H. Sajid, F. Ullah, K. Ayub, T. Mahmood, *J. Mol. Graph. Model.* **2020** , 97 , 107569.
- [53] H. Sajid, K. Ayub, T. Mahmood, *New J. Chem.* **2020** , 44 , 2609.
- [54] A. Shokuhi Rad, D. Zareyee, V. Pouralijan Foukolaei, B. Kamyab Moghadas, M. Peyravi, *Mol. Phys.* **2016** , 114 , 3143.
- [55] A. Shokuhi, K. Ayub, *J. Mol. Liq.* **2017** ,238 , 303.
- [56] M.T. Baei, A. Soltani, S. Hashemian, H. Mohammadian, *Can. J. Chem.* **2014** , 92 , 605.
- [57] R. Bhuvaneswari, V. Nagarajan, R. Chandiramouli, *Struct. Chem.* **2020** , 31 , 709.
- [58] A. Soltani, M.B. Javan, M.T. Baei, Z. Azmoodeh, *J. Alloys Compd.* **2018** , 735 , 2148.
- [59] R. Bhuvaneswari, V. Nagarajan, R. Chandiramouli, *J. Inorg. Organomet. Polym. Mater.* **2020** . DOI:10.1007/s10904-020-01488-8
- [60] A. Ahmadi, S.F. Rastegar, N.L. Hadipour, *Phys. Lett. A.* **2014** , 1 , 3.
- [61] R. Bhuvaneswari, J. Princy Maria, V. Nagarajan, R. Chandiramouli, *Mol. Phys.* **2020**, 1725671.
- [62] M. Samadzadeh, S.F. Rastegar, A.A. Peyghan, *Phys. E Low-Dimensional Syst. Nanostructures.* **2015** , 69 , 75.
- [63] A.A. Peyghan, M. Noei, S. Yourdkhani, *Superlattices Microstruct.* **2013** , 59 , 115.
- [64] J. Beheshtian, M.T. Baei, Z. Bagheri, A. Ahmadi, *Appl. Surf. Sci.* **2013** , 264 , 699.
- [65] E. C. Anota, M. A. Alejandro, A. B. Hernández, J. J. S. Torres, M. Castro, *RSC Adv.* **2016** , 6 , 20409.
- [66] J.P. Maria, V. Nagarajan, R. Chandiramouli, *J. Inorg. Organomet. Polym. Mater.* **2019** . DOI:10.1007/s10904-019-01352-4

- [67] J.C. Ordaz, E.C. Anota, M.S. Villanueva, M. Castro, *New J. Chem.* **2017** .
- [68] H. Ullah, S. Bibi, A.A. Tahir, T.K. Mallick, *J. Alloys Compd.* **2017** , 696 , 914.